The Cryosphere Discuss., doi:10.5194/tc-2016-67, 2016
Manuscript under review for journal The Cryosphere
Published: 30 March 2016

The Cryosphere Discussions
Open Access
EGU

Spatio-temporal evolution of snow depth observed by time-lapse laser scanning in the Alps and in Antarctica

Ghislain Picard[1,2], Laurent Arnaud[1], Jean-Michel Panel[3], and Samuel Morin[3]

[1]UJF – Grenoble 1 / CNRS, Laboratoire de Glaciologie et Géophysique de l'Environnement (LGGE) UMR 5183, Grenoble, F-38041, France
[2]ACE CRC, University of Tasmania, Private Bag 80, Hobart, TAS 7001, Australia
[3]Météo-France – CNRS, CNRM UMR 3589, Centre d'Études de la Neige, Grenoble, France

Correspondence to: Ghislain Picard (ghislain.picard@ujf-grenoble.fr)

Abstract. Although both the temporal and spatial variations of the snow depth are usually of interest for numerous applications, available measurement techniques are either space-oriented (e.g. terrestrial laserscans) or time-oriented (e.g. ultrasonic ranging probe). Because of snow heterogeneity, measuring depth in a single point is insufficient to provide accurate and representative estimates. We present a cost-effective automatic instrument to acquire spatio-temporal variations of snow depth. The device comprises a lasermeter mounted on a two-axis stage and can scan ≈200,000 points over an area of 100–200 m^2 in 4 hours. Two copies, installed in Antarctica and in the French Alps, have been operating daily, unattended over 2015 with a success rate of 65% and 90% respectively. The precision of single point measurements and long-term stability were evaluated to be about 1 cm and the accuracy to be 5 cm or better. The spatial variability in the scanned area reached 7–10 cm (root mean square) at both sites, which means that the number of measurements is sufficient to average out the spatial variability and yield precise mean snow depth. With such high precision, it was possible for the first time at Dome C 1) to observe a 3-month period of regular and slow increase of snow depth disconnected from snowfalls and 2) to highlight that most of the annual accumulation stems from a single event although several snowfall and strong wind events were predicted by the ERA-Interim reanalysis. At last the paper discusses the benefit of the RLS solution compared to multiplying single-point sensors in the context of monitoring snow depth.

1 Introduction

Snow depth is one of the most important and basic characteristics of snow on the ground. Measurements and modeling of this variable is crucial for numerous applications, such as in hydrology (Lopez-Moreno et al., 2013), avalanche forecasting (Schweizer, 2003), meteorology (de Rosnay et al., 2012), and for sea-ice (Lecomte et al., 2011; Katlein et al., 2015) or permafrost research (Gisnås et al., 2015). Snow depth is commonly reported in operational databases and measured at research monitoring stations or occasionally in the field. Many techniques are available to measure or monitor snow depth, the most common being manual measurements with a stick (emergence or depth, see e.g. Fierz et al., 2009) and ultrasonic ranging probes (Ryan et al., 2008). Their inherent accuracy is of the order of 1 cm which is largely sufficient for most applications. Nevertheless, the vast majority of these measurements are representative of a small area, typically less than 1 m^2, corresponding

The Cryosphere Discuss., doi:10.5194/tc-2016-67, 2016
Manuscript under review for journal The Cryosphere
Published: 30 March 2016

to the footprint of the sensor or the "homogeneous" area around the stick, whereas the spatial scale of interest is usually much larger than this, ranging from the area of meteorological monitoring stations (hundreds of square meters) to that of catchments (from a few square kilometers).

Since the snow cover is in general heterogeneous at any scales from the small scale to the application scale, the actual uncertainty of the snow depth in a given area is much larger than the inherent accuracy of individual measurements and is primarily governed by the spatial variability in this area (Grunewald et al., 2013). This variability stems from a variety of processes. Snowfall repartition is not uniform (Scipión et al., 2013) because of the ground topography at meter to kilometer scales, vegetation and other obstacles. Wind transport tends to amplify heterogeneity because erosion and redeposition are sensitive to small initial differences in the snow properties. Sastrugi, dunes, and other wind-formed features are frequent and their formation is still not well understood (Filhol and Sturm, 2015). Metamorphic and melt processes can also contribute to the decrease or increase of the spatial variations (Cathles et al., 2014). All these processes are complex and interact with each other so that the spatial variability can only be approached using high-resolution atmospheric-snowpack coupled models (Mott et al., 2010; Vionnet et al., 2014). As a consequence, from the perspective of snow depth estimation with ground-based measurements, the spatial variability has to be considered as a random noise whose characteristics are largely unknown (Trujillo and Lehning, 2015). In some extreme cases such as on the Antarctic plateau, the mean annual accumulation (which is the snow depth change during a year) can even be smaller than the spatial standard variations of the distribution (Eisen et al., 2008; Libois et al., 2014). It means for instance that in one point, net ablation or accumulation higher than twice the annual value occur frequently (Petit et al., 1982; Libois et al., 2014). In any case, accurate snow depth estimate requires averaging many independent point measurements to reduce the impact of this noise. As minimizing the number of measurements is often of practical importance, a good knowledge of the spatial variability (i.e, the statistical properties of the noise) is required (Trujillo and Lehning, 2015).

Terrestrial laser scanning (TLS, Prokop, 2008; Deems et al., 2013) is a fast-developing tool to characterize the spatial variability of snow depth. Recent advances have allowed improved range and increased density of measurements (number of points per square meter) thus allowing to cover all the relevant scales from the small scale to the application one (Deems et al., 2013). Most studies have explored the rich spatial information content (e.g. Revuelto et al., 2014; Filhol and Sturm, 2015) but only used a few scans acquired at two or a few different dates (Deems et al., 2015). While this may be enough to estimate the seasonal peak accumulation or study snow redistribution processes and geomorphology of the surface (Revuelto et al., 2016), it is insufficient to capture the individual events that affect snow height over a season. The cost of these devices – about 100 times the price of a single ranging probe – and the constraints on the operating conditions make their deployment in the field for continuous monitoring relatively challenging. Nevertheless, this application is rapidly emerging (Hartzell et al., 2015) and it is expected that a few catchments will be instrumented in the coming years. A cheaper emerging alternative uses unmanned autonomous vehicle with on-board camera and an image processing technique known as Surface from Motion (SfM, e.g. Jagt et al., 2015; Nolan et al., 2015) to construct digital elevation models from multiple images. A snow depth map is then derived by differenciating a no-snow acquisition taken before or after the snow season like with the TLS. While the technique can not reach vertical accuracy of 1cm yet, the density of measurements and range are of the same order as those of modern TLS.

The Cryosphere Discuss., doi:10.5194/tc-2016-67, 2016
Manuscript under review for journal The Cryosphere
Published: 30 March 2016

Operating conditions are also constraining which limits the frequency as with TLS. The same approach can also be applied at a higher resolution (Nicholson et al., 2016) and seems promising for continuous monitoring.

The purpose of this paper is to introduce and evaluate the performances of a new instrument which, in terms of spatial range, acquisition frequency and cost, lies between the spatial-oriented techniques (TLS, SfM) and temporal-oriented techniques (ultrasonic and laser ranging probes). The initial aim of this development was to measure mean snow depth with accuracy approaching 1 cm at a temporal resolution adequate to capture precipitation and wind transport events, snow densification and melt. The final solution is able to scan areas of an hundred of square meters, every day, for a cost inferior to that of ten single ranging probes, or to a tenth of common TLS. The robustness is another important factor since our goal was to cover full snow seasons up to a year without attending the instrument, in the harsh Antarctic conditions. As this factor was a strong constraint and drove many of our technical choices, the instrument is called the Rugged LaserScan (RLS). Two copies have been built, the first one has been deployed at the Col de Porte alpine site in the French Alps (45°N and 6°E, 1325 m altitude) (Morin et al., 2012) during one the winter campaigns of the World Meteorological Organization - Snow Precipitation InterComparison Experiment (WMO-SPICE) project (winter season 2014 - 2015) with the specific aim of investigating the accuracy and value of the device compared to traditional ranging probes. The second has been set up at Dome C in Antarctica (75°S and 123°E) in December 2014 and has been operating most of the time for over one year until it was dismantled for maintenance and improvements. The specific objective was to resolve the snow accumulation processes at shorter temporal scales than those captured with readings of stake emergence like those conducted for many years using glaciological methods, such as the GLACIOCLIM network of stakes (Genthon et al., 2015).

The paper is organized as follows: Section 2 introduces the instrument along with the calibration and data processing developed to produce gridded surface elevation maps and snow depth. Section 3 presents an evaluation of the stability and accuracy of the system as well as the spatial resolution. Based on this knowledge of the performance, it then analyzes the snow depth time-series in terms of physical processes at both sites. Section 4 evaluates the benefit of this instrument compared to single ranging probes in the context of the estimation of the mean snow depth. The present paper focuses on this estimation and does not cover the wide scope of spatial information content of the dataset which will be addressed in future work.

2 Materials and method

2.1 Rugged LaserScan (RLS)

We developed a rugged low-cost laserscan able to operate in harsh conditions like those encountered at Dome C where temperature regularly falls under -70°C in winter. Despite milder temperature at Col de Porte, a mid-altitude French alpine sites, rain and occasional storms represent another specific challenge. To minimize the risk, we based this development on an industrial lasermeter (DIMETIX FLS-CH 10) that we have already tested for several years at both sites. The good performance, robustness and cost were found satisfying. To convert this device designed to take point measurements only into a 2D scanner, we mounted it on a two-axis stage which performs the rotations in zenith and azimuth as depicted in Figure 1.

The Cryosphere Discuss., doi:10.5194/tc-2016-67, 2016
Manuscript under review for journal The Cryosphere
Published: 30 March 2016

The lasermeter has several operating modes to choose from depending on the expected measurement rate and precision. We selected the FAST mode which offers a theoretical range accuracy of $\pm 2\,\mathrm{mm}$ (statistical confidence level of 95.4%) at a rate of up to $20\,\mathrm{Hz}$. This rate shall not be confused with the Pulse Repetition Frequency (PRF, Deems et al., 2013) which refers to the number of laser pulses fired in a second and individual range measurements. In fact, the PRF should be much higher than $20\,\mathrm{Hz}$, but is not specified by the constructor in our case. The on-board software is in charge of accumulating and averaging all individual measurements until the estimated accuracy reaches the specifications of the selected mode. For this reason, the effective rate at which the measurements are returned to the user is not fixed, and can decrease under $20\,\mathrm{Hz}$ in unfavorable conditions. Among them, the brightness of the environment was found, during our early tests, to be an important factor, probably because the photo-receiver becomes saturated or the laser return is weak relative to the background in outdoor conditions. By adding a band-pass optical filter at the laser operating wavelength ($650\,\mathrm{nm}$) on the optical window, we greatly improved the outdoor performances. In addition, collecting the scan at night (or when the sun is at the lowest in Antarctica) also tended to improve the effective measurement rate. The distance and reflectivity of the target are two other important factors controlling the measurement rate. The specifications indicate a maximum range of $65\,\mathrm{m}$ when the device is still. However, for moving targets – or equivalently when the laser spot moves with respect to the ground as in our application – this range is in practice largely reduced.

In our setup, the spatial resolution and the time to cover a given surface area depend on both the speed of the spot on the ground and the rate of measurements. With an optimal rate of $20\,\mathrm{Hz}$ and a target spatial resolution of $2\,\mathrm{cm}$, it takes nearly 4 hours to cover a surface area of $100\,\mathrm{m}^2$. In this case, the spot on the ground moves at $2\,\mathrm{cm} \times 20\,\mathrm{Hz} = 0.4\,\mathrm{m\,s^{-1}}$. Higher speeds have been tried to reduce the scan duration but the measurement rate tends to degrade and even abruptly drop from $0.8\,\mathrm{m\,s^{-1}}$ on, which completely cancel out any gain.

The scan accuracy (the accuracy of x, y and z) depends on several factors (Deems et al., 2013). The along-range accuracy of the lasermeter is $2\,\mathrm{mm}$ in ideal conditions, which, projected in terrain coordinates can be doubled at the maximum zenith angle of 62° used here. In addition, the accuracy depends on the spot size which is about $8\,\mathrm{mm}$ in diameter (in the cross range direction) at $10\,\mathrm{m}$ and $15\,\mathrm{mm}$ at $30\,\mathrm{m}$ according to the constructor specifications. Altogether we estimate that the accuracy in z, considering only the lasermeter errors and the value given by the constructor, could reach about $5\,\mathrm{mm}$. Actual performances are presented in Section 3.

The two-axis stage is composed of two identical reduced motors controlled by a feedback on the position. This feedback loop is implemented with an analog proportional–integral–derivative controller (PID controller). The accuracy in position is mainly determined by the quality of the potentiometer which converts the angular position in a resistance and the electronics to convert the resistance into a numerical value. The chosen potentiometer model is given for a linearity of 0.2% which over a rotation range of 45° corresponds to an accuracy of about 0.1°. To highlight that this value is significant for our application, a laserscan set up at $z = 4\,\mathrm{m}$ above ground and considering a zenith angle of 62°, this angular error would translate in $3\,\mathrm{cm}$ error on z. It is noteworthy that this error is constant in time and should have a limited impact on the snow depth measurements which are obtained by difference. The precision (i.e. the reproducibility in position between different acquisitions) depends on other factors. It is mainly determined by the noise level of the feedback loop and according to our measurements is of the order of

The Cryosphere Discuss., doi:10.5194/tc-2016-67, 2016
Manuscript under review for journal The Cryosphere
Published: 30 March 2016

0.03° corresponding to 0.4 cm (1 unitcm resp.) for a zenith angle of 45°(62°resp.). This is three-fold smaller than the accuracy but does not compensate by differencing. It remains within our target. Note that the analog-digital and digital-analog converters used to measure and command the position, have a 16-bit dynamic range and auto-calibration which is largely sufficient given the above-mentioned other sources of error.

2.2 Modes of acquisition

An embedded computer controls the stages and the lasermeter. Two different operating configurations have been implemented, respectively called "scan mode" and "spot mode".

In **scan mode**, the sequence starts by setting the zenith angle θ at its minimum (19.0°). The range is continuously measured by the lasermeter while the azimuth stage rotates from $\phi = -90.0°$ to +90.0° at a speed of $v_\phi(\theta)$. The zenith angle is then increased by a small increment $\Delta\theta(\theta)$ and the next arc is completed from +90.0° to -90.0°. This process is repeated until the zenith angle reaches the upper limit set to 62°. The speed $v_\phi(\theta)$ and the increment $\Delta\theta(\theta)$ vary as a function of θ in order to ensure a uniform resolution on the surface. Hence, the speed typically ranges from $8° \, s^{-1}$ at 20° to $4.2° \, s^{-1}$ at 62°. The increment ranges from 0.4° to 0.1°. With such parameters a scan is completed in 4 hours and comprises around 200 000 points. One scan is acquired every day, a balance between scientific relevance and lifetime of the laser.

The **spot mode** was developed to follow the evolution of snow depth with a higher temporal resolution and potential better accuracy than with the scan mode. This mode monitors a limited set of points which are specified at the beginning of the season by their (x, y) horizontal position. The measurement in spot mode consists in determining the angles (θ, ϕ) so that the laser spot hits the surface of the snow at the vertical of the point (x, y). Figure 1 shows the principle in the vertical plane. The azimuth is constant regardless of the actual snow depth and is easily calculated from x and y. In contrast, the zenith angle depends on the snow surface elevation z, which is unknown and is actually the value we want to measure. An optimization algorithm was implemented to iteratively minimize the horizontal distance between the target point (x, y) and the actual projection of the laser spot in the horizontal plane. This distance is given by $\left| r\sin(\theta) - \sqrt{x^2 + y^2} \right|$ where r is the range measured by the lasermeter and θ the actual zenith angle. Once this distance is minimized to within a specified tolerance (e.g. 2 cm), 100 measurements of the lasermeter and angles are accumulated and averaged with the aims of reducing the reproducibility error. The snow surface elevation z is then calculated with the same formulas as for the scan mode. To speed up the optimization process, the optimal angle θ is stored for every point and used as first guess for the next acquisition. In practice, this mode allows to sample one point in about 30 s depending on the convergence time of the optimization. We have used this mode at Col de Porte to monitor every 2 hours the snow depth of 64 points in the scanned area over the season, excepted when RLS operates in scan mode (20–24h UTC).

2.3 Deployment

Pictures of the set up are shown in Figure 2. At Col de Porte, the laserscan was installed on the meteorological tower of the site at 5.4 m above ground. At Dome C, such a big structure would perturb the wind flow and cause artificial accumulation and erosion in the scanned area. To limit these effects, we use a very thin structure (38-mm diameter vertical steel rod) and

The Cryosphere Discuss., doi:10.5194/tc-2016-67, 2016
Manuscript under review for journal The Cryosphere
Published: 30 March 2016

try to avoid wind drag by limiting the installation height to 3.0 m above the surface. The stability of the structure is indeed an important factor for the accuracy (Deems et al., 2015) and can be challenging over a long period. Any movement of the device, either a translation or a rotation, directly results in position errors in the scans. The most likely movement is tilting of the structure with consequence on both the orientation of the device and its horizontal position. We estimate that stability as small as 0.1° is required as it corresponds to about 2 cm bias for an installation height of 5 m. In addition,vertical movements can occur at Dome C because the structure is anchored in the snow. For this, we connected the rod holding the device to a square wood board of 0.3m^2 buried horizontally at a depth of about 1.5 m. The structure thus follows the vertical movement of the board, that is the densification of the snow as that depth. Since the rate of densification at such a depth is very low compared to the expected changes at the surface (accumulation, surface snow densification, ...), the sinking of the structure is negligible. The same approach is used to measure accumulation with stacks (e.g. Magand et al., 2007; Eisen et al., 2008).

To record any movements during the season, we employed two strategies: at Dome C where the snow accumulation is only a few centimeters a year, it was possible to install polystyrene spheres (14.7 cm in diameter) in the field of view of the RLS about 20-cm above the surface. The spheres were mounted on a stick which was anchored into the snow at about 30-cm depth using a small plastic board following the same principle as for the structure. The spherical shape was chosen because the estimation of their center position from scans can be very robust even with an irregular number of points. Following the (x, y, z) position of the sphere centers allows to monitor the overall stability of the scanner including the structure, the stages, and lasermeter. Sinking of all the spheres and structure at the same rate would be undetectable but is unlikely. At Col de Porte, spheres were installed at the beginning of the season to check the horizontal leveling of the RLS but they were removed before the first snow because they would be buried during the season and may disturb the accumulation pattern. Instead, we installed a two-axis inclinometer on the RLS, to record the changes of inclination.

2.4 Data processing

The procedure to compute the position of the points in the (x, y, z) coordinates system from range measurements and stage angles is similar to any TLS and is briefly recalled here with emphasis on some RLS-specific details. It consists in the following steps:

1. The lasermeter returns measurements only when a satisfying quality is estimated by the on-board proprietary software, which ensures that the number of unrealistic or inaccurate measurements is limited. Nevertheless, additional checks are needed. A first filter is applied to remove too short ranges (<3 m) and too long ones (>17 m). A second filter further tracks outliers once the data are projected in (x, y, z) (see below).

2. The position of the spot in the (x, y, z) coordinate system is calculated as follows:

$$z = -r\cos\theta + \Delta_r \sin\theta \qquad r_{xy} = r\sin\theta + \Delta_c \cos\theta \qquad x = r_{xy}\cos\phi \qquad y = r_{xy}\sin\phi \tag{1}$$

where θ is the zenith angle (laser beam relative to the vertical), ϕ is the azimuth angle, and r is the range measured by the laser. Δ_r (respectively Δ_c) are the distance between the point for which $r = 0$ (close to the window of the laser) and the

The Cryosphere Discuss., doi:10.5194/tc-2016-67, 2016
Manuscript under review for journal The Cryosphere
Published: 30 March 2016

center of rotation of the laser projected along (resp. perpendicular to) the beam direction. r_{xy} is the range in the (x, y) plane.

3. Based on an estimate of the leveling of the laserscan (see below), a rotation $\mathcal{R}$ is applied to ensure that the (x, y) plane is perfectly horizontal. In addition, the z coordinate is shifted for convenience so that the origin $z = 0$ is at the mean ground level (for Col de Porte) and on a reference plane (for Dome C) instead of at the center of rotation of the laser which is meaningless.

4. The second filter is then applied. It considers that any point higher or lower by 5 cm from the mean height of its neighbors is removed. The neighborhood is taken as the disk in the horizontal plane of 5 cm in diameter centered at the tested point. This filter is efficient to remove outliers and thin objects like blowing flakes or the cables used to hang the structure. However, it can also erroneously remove areas with a summit or hollow if the local slope is abrupt (over 45°). At last, permanent artifacts in the scanned area (stacks, spheres, ...) are removed with specific ad hoc criteria.

5. The surface formed by the points (x, y, z) is resampled on a regular grid using the bilinear interpolation implemented in matplotlib.mlab.griddata Python library (version 1.5.1). The same grid is used throughout the season allowing easy calculation of the snow depth and other statistics with weighting. This approach is simple but may degrade the resolution compared to mesh based approaches (Deems et al., 2013). The chosen spacing was 2 and 3 cm at Col de Porte and Dome C respectively, reflecting the difference of installation height.

The procedure requires a few site-specific inputs, i.e. the rotation matrix and the reference plane. To determine the rotation, we installed four spheres in the scanned area and used a professional laser level to ensure they were in the same horizontal plane with an accuracy estimated to be $\pm 5\,\mathrm{mm}$. The position of each sphere was determined by first selecting only the points of the scan that reasonably lay in the sphere vicinity based on its expected position (first guess), and then minimizing the norm-1 of the function measuring the distance between the points (x, y, z) and the sphere surface: $\sqrt{(x-x_c)^2+(y-y_c)^2+(z-z_c)^2} - R$ where $R = 7.3\,\mathrm{cm}$ is the known sphere radius and (x_c, y_c, z_c) is the unknown sphere center in the unrotated coordinate system (obtained after step 2). The minimization uses the Random Sample Consensus algorithm (RANSAC, Fischler and Bolles, 1981) to automatically detect and remove outliers. A plane is then fitted onto the four spheres centers by least square fitting and the rotation R which puts this plane horizontal is deduced using the Cloud Compare software. The rotation angle was found to be 0.5° at both Dome C and Col de Porte demonstrating that the leveling of the laserscan mounting was good.

Once rotated, the $z = 0$ reference was taken at the mean elevation of the gridded data for the first scan taken at Dome C (1 January 2015), and for the average of all scans in the snow-free period between 9 and 16 November 2014 at Col de Porte.

2.5 WMO-SPICE data at Col de Porte

For the evaluation of the RLS, we use data collected in the framework of the WMO-SPICE experiment at Col de Porte. Two fixed lasermeters, OTT/Lufft/Jenoptik SHM 30.11 and Dimetrix FLS-CH 10 were used during the season. They were both set up on the same structure as RLS but shifted by a 2-m long horizontal arm. The lasermeter were tilted by about 20° from

The Cryosphere Discuss., doi:10.5194/tc-2016-67, 2016
Manuscript under review for journal The Cryosphere
Published: 30 March 2016

the vertical so that the measured footprint was not perturbed by snow accumulating on the arm and sensors and occasionally falling down or melting. However, with such an angle, the footprint position in the horizontal plane moves during the season as a function of the snow depth. It will be shown to be a limitation for the comparison with RLS data. The two snow depth time-series were calculated using range measurements, the tilt angles precisely measured for each sensor, and the offsets determined using the snow-free period :

$$d_{\mathrm{Dimetix}} = 4.2603 + 0.92666 \times r_{\mathrm{Dimetix}} \quad (2)$$

$$d_{\mathrm{Jenoptik}} = 4.2835 + 0.93643 \times r_{\mathrm{Jenoptik}} \quad (3)$$

.

Measurements were carried out every minute during the entire period of operation of the RLS at Col de Porte. For the needs of the WMO-SPICE experiment, the location of these sensors was chosen in an area of the experimental site known to feature generally very low natural variability of snow depth, based on visual inspection over the years. The goal was to concentrate on the possible measurement differences between the instruments tested, which could be due to the instruments themselves.

3 Results

The evolution of snow depth (mean and standard deviation) at Col de Porte and of surface elevation, i.e. snow depth with respect to the horizontal reference plane, at Dome C is shown in Figures 3 and 4. In order to provide an unbiased geophysical interpretation of these variations and distinguish spurious trends from actual variations, which is the ultimate goal of this section, it is necessary to assess in detail the performance, accuracy and precision of the RLS. To this end, we first describe the periods of operation and discuss the causes of failure (Section 3.1), then the stability of the instrument and the structure supporting it (Section 3.2) and the accuracy in spot and scan mode (Section 3.3). The spatial resolution is estimated in Section 3.5. Eventually, Section 3.6 provides the geophysical interpretation with a knowledge of the limitations.

3.1 General operating results

The Col de Porte scans were acquired from 7 October 2014 to 3 May 2015 (207 days) with a success rate of 90%. The snow period started with first ephemeral snowfall on 4 November 2014 and ended on 22 April 2015 when snow was completely absent from the scanned area. At Dome C, the time-series ranges between 1 January 2015 to 11 January 2016 when the device was dismantled. A major interruption occurred from 17 October 2105 to 5 December (49 days). Reports of the laser internal temperature indicated dysfunction of the internal heating. After a power shutdown from the Concordia station, it started to work again but the stability of the laser temperature was degraded compared to the first period (not shown). Considering that the lasermeter is given for a minimum operating temperature of -40°C and that it was exposed for several months to less than -70°C, it is possible that the lifetime of the heating element and control electronics was shortened. We can not however conclude that it is the cause of failure based on this single incident. Overall, the success rate over the period is 65%, and 75% when excluding the long interruption period in Austral spring.

The Cryosphere Discuss., doi:10.5194/tc-2016-67, 2016
Manuscript under review for journal The Cryosphere
Published: 30 March 2016

At both sites, the main cause of failure (after the major interruption at Dome C) is the jamming of the stages either because snow accumulated in the cap housing the device or maybe because ice could form on the heated motors. Since Dome C conditions were windier than Col de Porte and RLS is set up at a lower height than at Col de Porte, the occurrence and impact of blowing snow may be higher, contributing to the lower success rate. In addition, the lower temperature lengthens the recovery time after such event because of the slower sublimation. The second longest interruption at Dome C from 5 to 16 July following a large accumulation event is very likely to be caused by this problem. Snow or frost on the laser window is another issue, and were the likely cause of a few short interruptions (the lasermeter reports the "out of range" error in this case). They were rapidly cleared, in one or two days, thanks to the lasermeter heating.

3.2 Stability

3.2.1 Dome C

The stability of the RLS instrument and setup is evaluated at Dome C using the four spheres installed in an horizontal plane at the beginning of the season. Figure 5 shows the three coordinates of the spheres. Until the event of July 2014, the spheres were detected in nearly every scan. The time-series features a few abrupt variations of the order of 3 – 4 cm and slow trends of up to 1 cm. From July 2015 onwards, the series becomes discontinuous not only because of the failures of the RLS described in the previous Section, but also because the spheres were entirely (sphere #2) or partially buried (the three others). No other abrupt changes are observed during the second period and the trends seem to remain small, of the order of 1 cm.

In general, the timeseries depict complex variations which are difficult to understand in term of movements of the structure or the spheres. For instance the first series of changes in January visible in z could be interpreted as a lateral tilting of the structure (two spheres sink while the two other raise), but the absence of significant change in δx and δy at the same time invalidates this hypothesis. Sinking of the spheres due to the densificiation (the sphere are "anchored" at only 20–30 cm depth) is another possible hypothesis at this time of the year but it fails to explain why the sphere #2 is apparently raising. The sudden and large change experienced by sphere #1 during a wind event in March has the signature of a lateral movement of the sphere itself. At last, slow variations of the elevation $\delta' z$ of sphere #1, #3 and #4 are visible from February to July and seems to reverse from July to January. This could be due to a thermal effect (e.g. dilation of the structure). We also identified periods with hoar forming on the spheres (Champollion et al., 2013) that would result in a positive bias of the z coordinate of the spheres. This highlights the limit of using the spheres as a calibration system.

Nevertheless, despite these uncertainties, the amplitude of the variations gives an higher bound of the stability, and appears to be acceptable. For the snow depth, the most relevant is the vertical movements of the spheres which remain within 1 cm over the year if the period of settling after the installation is excluded (January 2015). This is small and acceptable but not negligible compared with the variations depicted in Figure 4.

The Cryosphere Discuss., doi:10.5194/tc-2016-67, 2016
Manuscript under review for journal The Cryosphere
Published: 30 March 2016

3.2.2 Col de Porte

In the absence of spheres, the stability at Col de Porte is evaluated using the 2-axis inclinometer fitted on the laserscan. Figure 6 shows the daily variations along the two axis (calculated by the daily median of the 5-minute acquisitions when the scanner is not running). The time-series reveals a shift occurring the 3 November 2014 before the first snowfalls. It is most probably due to a maintenance operation on the tower and implies to discard the data before this date which is not a problem because there are several available snow-free scans after this date.

From 3 November and until the end of the season, the day-to-day variations are of the order of 0.6° on the two axis (specifications of the sensors indicate an accuracy of 0.2° at -10°C). The long term trend is of the order of a decrease of 0.02° on both axis (too small to be visible in the Figure) which is only slightly larger than the long term stability of 0.01° given by the constructor. The impact of such a trend on the surface is of the order of $8\,\mathrm{mm}$ in the worse case at 62° zenith angle ($5.2(\tan(62°+0.02°)-\tan(62°))=0.008$). This is weak but highlights the need to take precaution on the laserscan mounting as it could be a significant part of the uncertainty budget (Deems et al., 2015).

3.3 Evaluation of the accuracy in spot mode

The comparison between RLS spot mode data to the two fixed lasermeters is presented in Figure 7. The overall variations of snow depth are very similar between the four curves indicating weak spatial variations between the two points (separated by about $1\,\mathrm{m}$) as well as weak differences between the lasermeters and RLS. The differences are more apparent on the residual plot in Figure 7. They range between $\pm 5\,\mathrm{cm}$ and vary by 1.0 and 1.8 cm RMS over the season for the Jenoptik and Dimetix points respectively. They show both rapid and slow variations, with an overall negative bias during the the accumulation period for both points, and a positive bias during the melt period for the Dimetix point only.

Different causes explain these two types of variations. The slow variations seem to be deterministic and could be explained by the slightly different point measured by the sensors. In fact, because of the constant tilt of the fixed sensors, the position of measured point on the surface moves toward the sensors (i.e. to the left in Figure 8) as the snow depth increases whereas RLS in spot mode measure exactly the same point (x,y) throughout the season. The distance between the measured points when the snow depth is maximum reaches about $60\,\mathrm{cm}$. By looking at the scans we indeed found variations over this distance range of the order of a few centimeters (Fig. 8) with a slope opposite to the sensors which matches the negative bias. Nevertheless, the precise trajectory of the points measured by the lasermeters is not known which prevents to further explore this hypothesis.

The rapid variations on the other hand are relatively random. This suggests they come from reproducibility errors of the sensors. The mean weekly standard difference of the 2 hourly data is about 0.4 and $0.7\,\mathrm{cm}$ for Jenoptik and Dimetix points on average over the season. The mean daily standard difference is about $0.3\,\mathrm{cm}$ for both points. These values are very low and should be compared to the 2-σ accuracy of the lasermeter of about $0.3\,\mathrm{cm}$ according to the constructor specification. The RLS angle reproducibility error was estimated to 0.03° which is sufficient to explain $0.5\,\mathrm{cm}$ RMS (evaluated for a zenith angle of 45° and a laserscan height of $5.2\,\mathrm{m}$).

The Cryosphere Discuss., doi:10.5194/tc-2016-67, 2016
Manuscript under review for journal The Cryosphere
Published: 30 March 2016

As a conclusion, we estimate the spot mode allows a sub-centimeter reproducibility for a measurement rate of about 2–3 min^{-1}. With our experimental setup, we are only able to provide an upper bound on the accuracy of the order of a few centimeters (precise value depends on the metrics, max or RMS differences). A more precise evaluation would require to compare the depth at exactly the same points over the season. In addition, it would be interesting to use complementary measurement technique because systematic errors due to the lasermeter technique are not taken into account in our evaluation, most notably the penetration depth of the laser in the snow. We expect this error to be small and rather constant of the order of 1 cm (Deems et al., 2013) or lower (Prokop, 2008). As this error does not concern the ground scans, it would tend to low bias all the snow depth measurements at Col de Porte while Dome C is not affected.

3.4 Evaluation of the accuracy in scan mode

To perform the comparison with the fixed sensors data following a similar approach to that of the previous section, we estimated for each scan the z coordinate at constant positions in the horizontal plane (x, y). To do so, we used the same interpolation method as for generating the regularly gridded product (Section 2.4) but interpolated at the points monitored in spot mode instead of on the regular grid (the difference would not be more than the grid spacing of 3 cm). In addition, only the fixed sensor data taken simultaneously with the scans (i.e. 20h -24h UTC) were considered to avoid differences emerging during ongoing snowfalls. The results in Figure 9 show very similar evolution of the snow depth for the three types of sensors as noted in spot mode. The daily residual ranges from -8 cm to +3 cm and is on average 1.2 and 2.3 cm RMS at Jenoptik and Dimetix points, similarly to that observed in spot mode. The variations of the residual is also a superposition of a slow component relatively well correlated to the snow depth, and rapid variations. The mean weekly standard difference is 0.5 and 0.8 cm at Jenoptik and Dimetix points respectively which is nearly as good as in spot mode. This is unexpected because the latter mode averages hundred single measurements at the same place whereas the former is based on interpolation involving 4 points at most. We conclude that the spot mode unnecessarily oversamples the surface and the number of measurements per point could be reduced hence allowing to monitor either more points or more frequently.

Overall this comparison shows that the RLS in scan mode provides similar measurement performances to the fixed sensors or the spot mode even when evaluated in single points. It means that further reduction of the random errors can be obtained by averaging the points over an area.

3.5 Evaluation of the effective spatial resolution

The spatial resolution is an important parameter when not only the mean snow depth but other characteristics of the surface are of interest, such as the distribution of snow depth, roughness, slope, etc. The theoretical spatial resolution can be estimated from scanning parameters (Section 2). In the cross-range direction (when the azimuth varies), it is 1.3 cm for the Col de Porte (RLS at 5.2 m height) and 0.7 cm for Dome C (RLS at 3.0 m height). In the range direction, the $\Delta\theta$ increment corresponds to 4.1 cm at the Col de Porte and 2.4 cm at Dome C. Since the increment and azimuth speed are appropriately scaled as a function of the zenith angle during the scan, the theoretical resolution in each direction is constant over the scanned area.

The Cryosphere Discuss., doi:10.5194/tc-2016-67, 2016
Manuscript under review for journal The Cryosphere
Published: 30 March 2016

The effective resolution should differ because of the angle reading errors, the lasermeter range error, and the lasermeter measurement rate. It is interesting to evaluate the resolution directly from the scans rather than from the theory. However, this is not straightforward because data are not acquired on a regular grid as highlighted in Figure 10 which shows the scans of 15 February 2015 at both sites as examples.

The number density of points measurements over the scanned area is about 3100 and 5200 m^{-1} at Col de Porte and Dome C respectively for this date which corresponds to points every 1.8 and 1.4 cm on average if the grid were rectangular and regular. However, because of the cross-range direction over-sampling, these distances are of little interest. The average distance between successive acquisitions (in azimuth) is easy to compute and is 0.9 cm on average at both sites which gives an estimate of the cross-range resolution. This agrees with the theoretical value considering that the measurement rate can vary around 20 Hz. Combining theses values and number density of points gives a first estimate of the resolution in the other direction. Results are 3.6 cm at Col de Porte and 2.1 m at Dome C which is slightly better than the theoretical value. However, Figure 10 highlights the irregularity of the zenith increments which we believe to come from the mechanics of the zenith stage and its feedback loop. As a result, the resolution in the zenith direction is irregular and distance between successive zenith increments ranges from 0 cm (i.e. superposition) up to 5 cm at Dome C and 7 cm at Col de Porte in the area covered in Figure10. These latter values give an upper limit on the resolution and can be used as conservative estimates.

3.6 Analysis of the evolutions of snow depth and accumulation

3.6.1 Col de Porte

The evolution of the snow depth depicted in Figure 3 is representative of an Alpine mid-altitude site. It features a period of accumulation with significant snowfall building up a snowpack up to a depth of 1.46 m (Fig. 8). It is followed by an overall decrease due to the accelerated compaction and melt of the snowpack. With such large accumulation values compared to the precision estimated in Section 3.4 and the number of points in the scan (over 150,000), the statistical and instrumental relative errors are always small. The variations of the mean snow depth can be attributed with confidence to physical processes. Even the three ephemeral snowfall events that occurred at the beginning of the season with maximum snow depth (observed at 20h UTC) of 8 cm (4 November 2014), 8 cm (17 November 2014) and 16 cm (8 December 2014) are well described. The standard deviation of snow depth over the scanned area (hereinafter σ_s) is of the order of 1.2 – 1.7 cm for the three events. As it is close to the reproducibility estimated in Section 3.4, we can postulate that the true standard deviation of the snow height is probably smaller than 1.2 cm, that is, the snow depth is very homogeneous. The three next snowfall events show a similar behavior, despite larger accumulation. Over the accumulation period the standard deviation remains inferior to 4 cm until the maximum is reached on 26 February 2015.

A rain on snow event occurred on 1 March 2015 marking the beginning of the melt season. Four days later, a windslab was formed in the Northern corner of the scan ($y \approx +6\mathrm{m}$ in Fig. 8). This resulted in a sharp increase of the snow depth standard deviation, up to 10 cm, which remained high around 8 cm until 22 April 2015, a few days only before the scanned area became entirely snow free. Since the windslab is only partially viewed by the RLS, the interpretation of the standard deviation value

The Cryosphere Discuss., doi:10.5194/tc-2016-67, 2016
Manuscript under review for journal The Cryosphere
Published: 30 March 2016

is delicate. Indeed, from a statistical point of view, the snow depth field is not stationary over the sampled area and while statistical estimators can always be computed, they may be over-sensitive to the choice of the sampled area, and eventually become useless. This also concerns statistical tests and other frameworks that rely on the assumption of stationarity (Trujillo and Lehning, 2015) and may fail more frequently than predicted by theory. While in practice it is desirable to observe the snow depth field at a large scale to ensure the stationarity, it is not always easy to achieve. It was indeed impracticable in our case not only because of the limited range of the RLS (limited by the lasermeter and by the height of installation), but also because of the size of the Col de Porte site. The site is relatively sheltered compared to higher altitude sites and the area selected for the WMO-SPICE experiment was flat and relatively clear from obstacles. Our results regarding the homogeneity during the accumulation period support a posteriori the choice of this particular area to conduct the WMO-SPICE inter-comparison of snow depth sensors. Nevertheless, a few trees, the main building of the site and the fence are about only 10 m from the scanned and SPICE area, which makes vain to reach stationarity of the snow depth scale. Fortunately, the windslab – probably formed due to the presence of the trees and the fence – did not expand up to the WMO-SPICE sensor footprints.

3.6.2 Dome C

The evolution of the accumulation is radically different at Dome C (Figure 3). The mean accumulation over the season amounts to only 8 cm which is expected. It corresponds to the annual mean at this site (Petit et al., 1982) and is of the same order as the measurements on the GLACIOCLIM stack network (orange points in Figure 4) averaging to 6.4 cm over a similar period.

More surprisingly, the time-series shows that most of the annual accumulation comes from a single deposition event happening between the 5 and 17 July 2015, most likely at the beginning of this period because we believe it to be responsible of the failure of the instrument. ERA Interim reanalysis data (Dee et al., 2011) confirm this hypothesis. It is well known that the deposition is mainly driven by wind on the Antarctic Plateau (Groot Zwaaftink et al., 2013; Libois et al., 2014) and it was shown that, from a modeling perspective, it is more accurate to accumulate precipitation in a virtual reservoir and empty it on the snowpack when some criteria on the wind speed are met than to accumulate precipitation as and when they fall, as it is common in the Alpine regions. Nevertheless, our observation is more extreme than suggested by the previous studies (Groot Zwaaftink et al., 2013; Libois et al., 2014). We estimate that over the period more than 6 significant snowfalls and a dozen of strong wind events (here $> 8 \mathrm{mms}^{-1}$) predicted by ERA Interim reanalysis (lower panel in Figure 4) could have caused a significant accumulation but did not. Whether this new observation is a rare event, or common, or is biased by the relatively limited scanned area, is an open but important question. Only a longer time-series of observations could provide further insights.

In addition to this particular event, the series shows other remarkable patterns of variations, particularly visible during the first part of the series. From February to July, the snow elevation shows two periods of slow and regular increase separated by an erosion event occurring ca. 20 March. During each period approximately 2.5 cm have accumulated and the erosion event removed 2 cm in one or two days. Based on the analysis of the stability (Section 3.2) and accuracy (Section 3.4), we are confident these are real. Such periods of slow accumulation have already been suggested by Picard et al. (2012) based on indirect inferences using microwave remote sensing observations. The 12 year long time-series of satellite data even suggests

The Cryosphere Discuss., doi:10.5194/tc-2016-67, 2016
Manuscript under review for journal The Cryosphere
Published: 30 March 2016

that most of the accumulation in winter is due to this slow process, which is not captured by the ERA reanalysis. This could be explained by clear-sky precipitation (Walden et al., 2003), hoar growth and/or condensation (Champollion et al., 2013). The rapid erosion event is associated with a strong wind in the reanalysis, however it is worth noting that wind speeds over $8\,\mathrm{ms}^{-1}$ are present throughout the period of observations but they did not result in erosion. The direction of the wind and pre-existing conditions in the near-surface snowpack are probable factors governing the erosion.

The small temporal evolutions are revealed because many points are averaged. The spatial variability in the scanned area is indeed significant and changes over the time-series. In absolute value, it is of the same order as in Col de Porte with $\sigma_s = 3.5\,\mathrm{cm}$ RMS in the beginning of the season and $\sigma_s = 7\,\mathrm{cm}$ RMS in the end. However in relative value, it is about 0.5 – 1 times the mean annual accumulation whereas at Col de Porte it never exceeds 0.05 of the maximum accumulation.

Since the surface shape frequently changes due redistribution, it implies that the annual accumulation measured in any point is highly variable around the mean. It can even be negative at some point, a case called accumulation hiatus (Courville et al., 2007; Das et al., 2013; Libois et al., 2014). Figure 11 shows the distribution of annual accumulation from RLS over the scanned area together with that calculated from the GLACIOCLIM 50-stakes network near Concordia. The investigated periods are slightly different due to the availability of the data but are comparable (3 January 2015 to 18 November 2015 for GLACIOCLIM and to 5 December 2015 for the RLS, as it is the closest RLS acquisition after the GLACIOCLIM measurement). The distributions are similar except a general positive offset for RLS which corresponds to the difference visible on the time-series in Figure 4 between the two spring acquisitions. This similitude is remarkable considering the much smaller area covered by the RLS and the distance between the two sites (about $2\,\mathrm{km}$). It highlights the potential to explore new ranges of spatio-temporal scales using time-lapse laserscanning.

4 Discussions

We have demonstrated that the RLS is able to measure snow depth over a very large number of points with comparable accuracy as with single point sensors. By averaging the spatial variability over these points, the RLS can thus provide mean snow depth over an area of the order of hundred of square meters with a precision approaching the intrinsic precision of the sensor, i.e. about $1\mathrm{cm}$. To evaluate the value of the RLS concept regarding snow depth estimation in a fair way, other factors need to be taken into account. The question is in fact whether a network of N point sensors with an identitical overall "cost" could provide the same accuracy or not. The term "cost" here is open and includes different aspects including device price, maintenance, logistical constraints, robustness and risks. This question is closely related to that of designing snow depth survey from manual measurements (snow course) or equivalently determine the number (and location) of measurements needed to reach some accuracy level. This has been extensively highlighted e.g. by Grunewald et al. (2013) and investigated in detail by Trujillo and Lehning (2015) using a geospatial statistical framework. However, to apply it in our case is not straightforward because the spatial signal has been shown not to be stationary at both Col de Porte (windslab) and Dome C (slope). Nevertheless it is possible to obtain similar statistical results by picking random samples from the observed scans, which assumes ergodicity and negligible spatial correlation. Practically, we consider that N point sensors are randomly located in the scanned area and

The Cryosphere Discuss., doi:10.5194/tc-2016-67, 2016
Manuscript under review for journal The Cryosphere
Published: 30 March 2016

compare their averaged snow depth to the true snow depth estimated by the average over the whole scanned area. An example for $N = 6$ at Dome C is shown in Figure 12 along with the independent time-series acquired by an ultrasonic ranging probe located about 10 m from the RLS. While the individual trajectories are tangled and each one depicts a particular story about the snow accumulation in 2015, the 6-point mean looks similar to the scan mean (i.e. true value). Nevertheless it quantitatively differs. The difference gives an estimate of the error ε due to the limited number of observed points. For a large number of random sampling and for different N, we found that the rules $\varepsilon = \sigma_s/\sqrt{N}$ precisely applies despite the non stationarity and possible correlation. As a result, based on standard deviation σ_s given in Sections 3.6.1 and 3.6.2, we can estimate that a network of $N = 5$ sensors (resp. $N = 10$) would have a 1-σ error of $\approx 3.5\,\mathrm{cm}$ (2.5 cm) which is quite large compared to the centimeter precision of the RLS. To attain an error of 1.5 cm (resp. 1 cm), 30 (60 resp.) sensors are necessary. We also should emphasize that these values of error may be over-optimistic as Trujillo and Lehning (2015) found large increases of the standard variation as a function of the size of the covered area, typically 2 to 5-fold between 10 m (the scale of the RLS range) and 100 m because of long-range correlation.

In any case, this demonstrates that a single sensor or a small network is unable to approach the centimeter accuracy and that the spatial variability always dominates the error budget with current sensor technology. While the centimeter accuracy may be inessential for Alpine regions, the detection at Dome C of the slow accumulation periods and the zero net accumulation during all but one snowfalls and strong wind events definitely relies on the ability to average the spatial variability.

Furthermore, the cost of a N-sensor network generally increases with N while the gain in accuracy only follows $\sqrt{N}$. The RLS comes with a higher but fixed cost and provides a large number of points that is sufficient to reduced the error due to the spatial variability to negligible levels. Nevertheless, the current design of RLS provides a limited range which is insufficient to capture some interesting spatial scales (Picard et al., 2014; Filhol and Sturm, 2015; Trujillo and Lehning, 2015) and could become an issue when long-range spatial correlations are important. While the installation height could be increased by a few meters to improve this – especially at Dome C where it was only 3m – some characteristics of the lasermeter (maximal range and measurement rate) and the precision of the stages are intrinsically limited. In this domain, the recent commercial laserscans outperform the RLS.

5 Conclusions

This paper shows that a lasermeter designed for snow depth point measurements can be transformed into an automatic, robust and low cost laserscan by adding a two-axis mechanical stage. About 200 000 points of measurements can be obtained daily, with a precision of the order of 1 cm, and in an area of 150 m^2 when the instrument is set up 5.5 m above the surface. With such a system, the mean snow depth of an area can be estimated with an accuracy approaching the intrinsic accuracy of the instrument, i.e. 1 cm. We estimated that this could not be obtained with a network of point sensors for a similar cost.

The variations of snow depth at Col de Porte over the winter season 2014 – 2015 is typical of Alpine regions, with a few ephemeral snowfalls, then a period of accumulation comprising about 6 heavy snowfall events, and at last a period of melt. At Dome C, the most remarkable result is that most of the accumulation amount over the year comes from a single event

The Cryosphere Discuss., doi:10.5194/tc-2016-67, 2016
Manuscript under review for journal The Cryosphere
Published: 30 March 2016

occurring in July. In addition, the time-series features periods of slow and regular accumulation without apparent "snowfall" in the meteorological data which points to "clear sky" precipitation, condensation or hoar formation.

Further works include improvements of the instrument and further analysis of the data. The rate of failure (mainly due to snow drift) needs to be improved, the power consumption could be optimized in order to make the instrument energy autonomous, and installation at greater height should be explored to increase the scanned surface area.

This study was focused on the instrument accuracy and the mean snow depth estimation for which the RLS is seen as a provider of numerous independent points of snow depth measurement. However, RLS provides, as any laserscan, maps, that is continuous field of surface elevation and depth whose spatial properties – and spatio-temporal properties for the RLS – are very rich and deserve further exploration. Applications of this new system encompass the study of accumulation process on a broad range of spatial and time scales, and the evolution of geometrical and aerodynamical roughnesses for application in remote sensing and surface turbulence.

In the broader context of the WMO-SPICE project, the development of the RLS demonstrates that escaping the limitations of automated point measurements of snow depth due to the spatial variability of the snowpack itself becomes possible only if a significant number (more than 10 typically) of observation are taken simultaneously at the same measurement point (let alone longer range variability which is particularly significant in mountainous terrain, see e.g. Grunewald et al., 2013. This development paves the way for future questions and potential operational implementation. In terms of snow depth data assimilation in meteorological or hydrological models, while it is well known that snowpack heterogeneity can be found in virtually all environmental contexts, single snow depth values are generally considered representative for given monitoring stations in the assimilation systems, and most often are deducted from a single sensor. Findings made possible by the RLS make it possible to envision the development of future snow monitoring devices which could approach the variability of snow depth at the monitoring station level and, more importantly, communicate along with the mean value a quantitative estimate of the spatial variability, which could be considered in the assimilation systems as an indication of the representativeness of the measured mean value. This requires that such measurement campaigns and analyses are repeated in various environmental contexts to assess to what extent the findings in this study apply broadly on all terrestrial land surfaces, and fully assess its implications in terms of the ability to monitor snow depth using single sensors.

Acknowledgements. This study was supported by the ANR program 1-JS56-005-01 MONISNOW and by a grant from OSUG@2020 (investissement d'avenir – ANR10 LABX56). The authors acknowledge the French Polar Institute (IPEV) for the financial and logistic support at Concordia station in Antarctica through the NIVO program. We thank Yves Lejeune, Erwan Le Gac, Jacques Roulle and Laurent Pezard for their help in setting-up and running observations at Col de Porte. We thank Eric Lefebvre and Bruno Jourdain for the installation of the laserscan at Dome C and the winter-over staff at Concordia for the maintenance. We thank Vincent Favier and Roxanne Jacob for providing the GLACIOCLIM emergence data. Snow measurements at Col de Porte and Dome C contribute to the SOERE CryObs-Clim observatory and the OSUG CENACLAM observation group. Some of the results presented in this work were obtained as part of the Solid Precipitation Intercomparison Experiment (SPICE) conducted on behalf of the World Meteorological Organization (WMO) Commission for Instruments and Methods of Observation (CIMO). The analysis described herein does not necessarily represent the official outcome of WMO-SPICE.

The Cryosphere Discuss., doi:10.5194/tc-2016-67, 2016
Manuscript under review for journal The Cryosphere
Published: 30 March 2016

Mention of commercial companies or products is solely for the purposes of information and assessment within the scope of the present work, and does not constitute a commercial endorsement of any instrument or instrument manufacturer by the authors or the WMO.

Author contributions. G. Picard and L. Arnaud developed and built the Rugged Laserscan (RLS). J.-M. Panel managed the lasermeters in particular and the Col de Porte infrastructure in general. S. Morin coordinated the work in framework of the WMO-SPICE campaign at Col de Porte. All the authors contributed to the evaluation and data analysis and prepared the manuscript.

The Cryosphere Discuss., doi:10.5194/tc-2016-67, 2016
Manuscript under review for journal The Cryosphere
Published: 30 March 2016

References

Cathles, L. M., Abbot, D. S., and MacAyeal, D. R.: Intra-surface radiative transfer limits the geographic extent of snow penitents on horizontal snowfields, Journal of Glaciology, 60, 147–154, doi:10.3189/2014jog13j124, http://dx.doi.org/10.3189/2014JoG13J124, 2014.

Champollion, N., Picard, G., Arnaud, L., Lefebvre, E., and Fily, M.: Hoar crystal development and disappearance at Dome C, Antarctica: observation by near-infrared photography and passive microwave satellite, The Cryosphere, 7, 1247–1262, doi:10.5194/tc-7-1247-2013, 2013.

Courville, Z. R., Albert, M. R., Fahnestock, M. A., Cathles IV, L. M., and Shuman, C. A.: Impacts of an accumulation hiatus on the physical properties of firn at a low-accumulation polar site, J. Geophys. Res., 112, F02 030+, doi:10.1029/2005JF000429, 2007.

Das, I., Bell, R. E., Scambos, T. A., Wolovick, M., Creyts, T. T., Studinger, M., Frearson, N., Nicolas, J. P., Lenaerts, J. T. M., and van den Broeke, M. R.: Influence of persistent wind scour on the surface mass balance of Antarctica, Nature Geoscience, 6, 367–371, doi:10.1038/ngeo1766, http://dx.doi.org/10.1038/ngeo1766, 2013.

de Rosnay, P., Balsamo, G., Albergel, C., Muñoz-Sabater, J., and Isaksen, L.: Initialisation of Land Surface Variables for Numerical Weather Prediction, Surveys in Geophysics, pp. 1–15, doi:10.1007/s10712-012-9207-x, 2012.

Dee, D. P., Uppala, S. M., Simmons, A. J., Berrisford, P., Poli, P., Kobayashi, S., Andrae, U., Balmaseda, M. A., Balsamo, G., Bauer, P., and et al.: The ERA-Interim reanalysis: configuration and performance of the data assimilation system, Q.J.R. Meteorol. Soc., 137, 553–597, doi:10.1002/qj.828, http://dx.doi.org/10.1002/qj.828, 2011.

Deems, J. S., Painter, T. H., and Finnegan, D. C.: Lidar measurement of snow depth: a review, Journal of Glaciology, 59, 467–479, doi:10.3189/2013jog12j154, http://dx.doi.org/10.3189/2013JoG12J154, 2013.

Deems, J. S., Gadomski, P. J., Vellone, D., Evanczyk, R., LeWinter, A. L., Birkeland, K. W., and Finnegan, D. C.: Mapping starting zone snow depth with a ground-based lidar to assist avalanche control and forecasting, Cold Regions Science and Technology, 120, 197–204, doi:10.1016/j.coldregions.2015.09.002, http://dx.doi.org/10.1016/j.coldregions.2015.09.002, 2015.

Eisen, O., Frezzotti, M., Genthon, C., Isaksson, E., Magand, O., van den Broeke, M. R., Dixon, D. A., Ekaykin, A., Holmlund, P., Kameda, T., and et al.: Ground-based measurements of spatial and temporal variability of snow accumulation in East Antarctica, Reviews of Geophysics, 46, doi:10.1029/2006rg000218, http://dx.doi.org/10.1029/2006RG000218, 2008.

Fierz, C., Armstrong, R. L., Durand, Y., Etchevers, P., Greene, E., McClung, D. M., Nishimura, K., Satyawali, P. K., and Sokratov, S. A.: The international classification for seasonal snow on the ground, UNESCO/IHP, 2009.

Filhol, S. and Sturm, M.: Snow bedforms: A review, new data, and a formation model, J. Geophys. Res. Earth Surf., 120, 1645–1669, doi:10.1002/2015jf003529, http://dx.doi.org/10.1002/2015JF003529, 2015.

Fischler, M. A. and Bolles, R. C.: Random sample consensus: a paradigm for model fitting with applications to image analysis and automated cartography, Commun. ACM, 24, 381–395, doi:10.1145/358669.358692, http://dx.doi.org/10.1145/358669.358692, 1981.

Genthon, C., Six, D., Scarchilli, C., Ciardini, V., and Frezzotti, M.: Meteorological and snow accumulation gradients across Dome C, East Antarctic plateau, Int. J. Climatol., 36, 455–466, doi:10.1002/joc.4362, http://dx.doi.org/10.1002/joc.4362, 2015.

Gisnås, K., Westermann, S., Schuler, T. V., Melvold, K., and Etzelmüller, B.: Small-scale variation of snow in a regional permafrost model, The Cryosphere Discussions, 9, 6661–6696, doi:10.5194/tcd-9-6661-2015, http://dx.doi.org/10.5194/tcd-9-6661-2015, 2015.

Groot Zwaaftink, C. D., Cagnati, A., Crepaz, A., Fierz, C., Macelloni, G., Valt, M., and Lehning, M.: Event-driven deposition of snow on the Antarctic Plateau: analyzing field measurements with SNOWPACK, The Cryosphere, 7, 333–347, doi:10.5194/tc-7-333-2013, http://dx.doi.org/10.5194/tc-7-333-2013, 2013.

Grunewald, T., Stotter, J., Pomeroy, J. W., Dadic, R., Moreno Banos, I., Marturia, J., Spross, M., Hopkinson, C., Burlando, P., and Lehning, M.: Statistical modelling of the snow depth distribution in open alpine terrain, Hydrology and Earth System Sciences, 17, 3005–3021, doi:10.5194/hess-17-3005-2013, 2013.

Hartzell, P. J., Gadomski, P. J., Glennie, C. L., Finnegan, D. C., and Deems, J. S.: Rigorous error propagation for terrestrial laser scanning with application to snow volume uncertainty, Journal of Glaciology, 61, 1147–1158, doi:10.3189/2015jog15j031, http://dx.doi.org/10.3189/2015JoG15J031, 2015.

Jagt, B., Lucieer, A., Wallace, L., Turner, D., and Durand, M.: Snow Depth Retrieval with UAS Using Photogrammetric Techniques, Geosciences, 5, 264–285, doi:10.3390/geosciences5030264, http://dx.doi.org/10.3390/geosciences5030264, 2015.

Katlein, C., Arndt, S., Nicolaus, M., Perovich, D. K., Jakuba, M. V., Suman, S., Elliott, S., Whitcomb, L. L., McFarland, C. J., Gerdes, R., and et al.: Influence of ice thickness and surface properties on light transmission through Arctic sea ice, Journal of Geophysical Research: Oceans, 120, 5932–5944, doi:10.1002/2015jc010914, http://dx.doi.org/10.1002/2015JC010914, 2015.

Lecomte, O., Fichefet, T., Vancoppenolle, M., and Nicolaus, M.: A new snow thermodynamic scheme for large-scale sea-ice models, Annals of Glaciology, 52, 337–346, doi:10.3189/172756411795931453, http://dx.doi.org/10.3189/172756411795931453, 2011.

Libois, Q., Picard, G., Arnaud, L., Morin, S., and Brun, E.: Modeling the impact of snow drift on the decameter-scale variability of snow properties on the Antarctic Plateau, J. Geophys. Res. Atmos., 119, 11,662–11,681, doi:10.1002/2014jd022361, http://dx.doi.org/10.1002/2014JD022361, 2014.

Lopez-Moreno, J., Fassnacht, S., Heath, J., Musselman, K., Revuelto, J., Latron, J., Moran-Tejeda, E., and Jonas, T.: Small scale spatial variability of snow density and depth over complex alpine terrain: Implications for estimating snow water equivalent, Adv. Water Resour., 55, 40 – 52, doi:10.1016/j.advwatres.2012.08.010, 2013.

Magand, O., Genthon, C., Fily, M., Krinner, G., Picard, G., Frezzotti, M., and Ekaykin, A. A.: An up-to-date quality-controlled surface mass balance data set for the 90°–180°E Antarctica sector and 1950–2005 period, Journal of Geophysical Research, 112, doi:10.1029/2006jd007691, http://dx.doi.org/10.1029/2006JD007691, 2007.

Morin, S., Lejeune, Y., Lesaffre, B., Panel, J., Poncet, D., David, P., and Sudul, M.: An 18-yr long (1993–2011) snow and meteorological dataset from a mid-altitude mountain site (Col de Porte, France, 1325 m alt.) for driving and evaluating snowpack models, Earth System Science Data, 4, 13–21, doi:10.5194/essd-4-13-2012, http://www.earth-syst-sci-data.net/4/13/2012/, 2012.

Mott, R., Schirmer, M., Bavay, M., Grünewald, T., and Lehning, M.: Understanding snow-transport processes shaping the mountain snowcover, The Cryosphere, 4, 545–559, doi:10.5194/tc-4-545-2010, 2010.

Nicholson, L. I., Pętlicki, M., Partan, B., and MacDonell, S.: 3D surface properties of glacier penitentes over an ablation season, measured using a Microsoft Xbox Kinect, The Cryosphere Discussions, p. 1–31, doi:10.5194/tc-2015-207, http://dx.doi.org/10.5194/tc-2015-207, 2016.

Nolan, M., Larsen, C., and Sturm, M.: Mapping snow depth from manned aircraft on landscape scales at centimeter resolution using structure-from-motion photogrammetry, The Cryosphere, 9, 1445–1463, doi:10.5194/tc-9-1445-2015, http://dx.doi.org/10.5194/tc-9-1445-2015, 2015.

Petit, J. R., Jouzel, J., Pourchet, M., and Merlivat, L.: A detailed study of snow accumulation and stable isotope content in Dome C (Antarctica), Journal of Geophysical Research, 87, 4301, doi:10.1029/jc087ic06p04301, http://dx.doi.org/10.1029/JC087iC06p04301, 1982.

Picard, G., Domine, F., Krinner, G., Arnaud, L., and Lefebvre, E.: Inhibition of the positive snow-albedo feedback by precipitation in interior Antarctica, Nature Climate Change, 2, 795–798, doi:10.1038/nclimate1590, 2012.

Picard, G., Royer, A., Arnaud, L., and Fily, M.: Influence of meter-scale wind-formed features on the variability of the microwave brightness temperature around Dome C in Antarctica, The Cryosphere, 8, 1105–1119, doi:10.5194/tc-8-1105-2014, http://dx.doi.org/10.5194/tc-8-1105-2014, 2014.

Prokop, A.: Assessing the applicability of terrestrial laser scanning for spatial snow depth measurements, Cold Reg. Sci. Technol., 54, 155–163, 2008.

Revuelto, J., López-Moreno, J. I., Azorin-Molina, C., and Vicente-Serrano, S. M.: Topographic control of snowpack distribution in a small catchment in the central Spanish Pyrenees: intra- and inter-annual persistence, The Cryosphere, 8, 1989–2006, doi:10.5194/tc-8-1989-2014, http://dx.doi.org/10.5194/tc-8-1989-2014, 2014.

Revuelto, J., Vionnet, V., Lopez-Moreno, J.-I., Lafaysse, M., and Morin, S.: Combining snowpack modeling and terrestrial laser scanner observations improves the simulation of small scale snow dynamics, J. Hydrol., 533, 291 – 307, doi:10.1016/j.jhydrol.2015.12.015, 2016.

Ryan, W. A., Doesken, N. J., and Fassnacht, S. R.: Evaluation of Ultrasonic Snow Depth Sensors for U.S. Snow Measurements, Journal of Atmospheric and Oceanic Technology, 25, 667–684, doi:10.1175/2007jtecha947.1, http://dx.doi.org/10.1175/2007JTECHA947.1, 2008.

Schweizer, J.: Snow avalanche formation, Reviews of Geophysics, 41, doi:10.1029/2002rg000123, http://dx.doi.org/10.1029/2002RG000123, 2003.

Scipión, D. E., Mott, R., Lehning, M., Schneebeli, M., and Berne, A.: Seasonal small-scale spatial variability in alpine snowfall and snow accumulation, Water Resour. Res., 49, 1446–1457, doi:10.1002/wrcr.20135, http://dx.doi.org/10.1002/wrcr.20135, 2013.

Trujillo, E. and Lehning, M.: Theoretical analysis of errors when estimating snow distribution through point measurements, The Cryosphere, 9, 1249–1264, doi:10.5194/tc-9-1249-2015, http://dx.doi.org/10.5194/tc-9-1249-2015, 2015.

Vionnet, V., Martin, E., Masson, V., Guyomarc'h, G., Naaim-Bouvet, F., Prokop, A., Durand, Y., and Lac, C.: Simulation of wind-induced snow transport and sublimation in alpine terrain using a fully coupled snowpack/atmosphere model, The Cryosphere, 8, 395–415, doi:10.5194/tc-8-395-2014, 2014.

Walden, V. P., Warren, S. G., and Tuttle, E.: Atmospheric Ice Crystals over the Antarctic Plateau in Winter, Journal of Applied Meteorology, 42, 1391–1405, doi:10.1175/1520-0450(2003)042<1391:AICOTA>2.0.CO;2, http://journals.ametsoc.org/doi/abs/10.1175/1520-0450%282003%29042%3C1391%3AAICOTA%3E2.0.CO%3B2, 2003.

The Cryosphere Discuss., doi:10.5194/tc-2016-67, 2016
Manuscript under review for journal The Cryosphere
Published: 30 March 2016

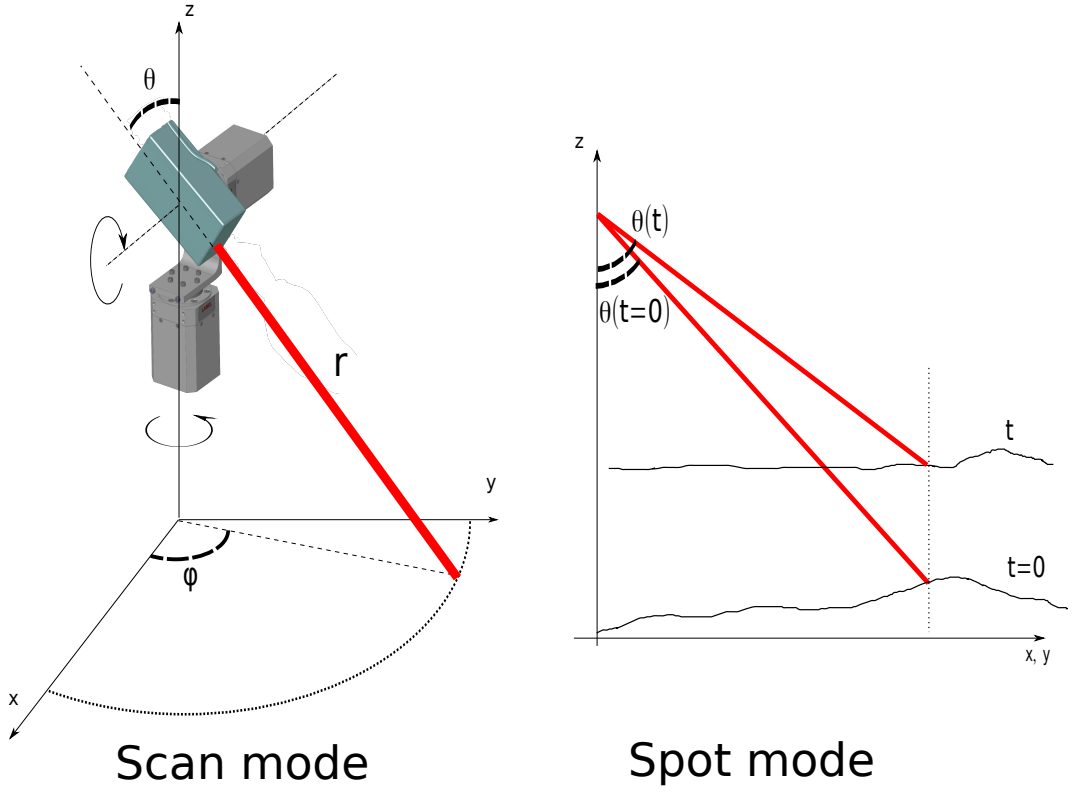

Figure 1. Principle of the scan mode and spot mode of the Rugged Laser Scan (RLS). The zenith angle θ and azimuth angle ϕ determines the orientation of the lasermeter which measures the range r.

The Cryosphere Discuss., doi:10.5194/tc-2016-67, 2016
Manuscript under review for journal The Cryosphere
Published: 30 March 2016

Figure 2. Pictures of RLS during the installation at Col de Porte (October 2014) and at Dome C (December 2014).

The Cryosphere Discuss., doi:10.5194/tc-2016-67, 2016
Manuscript under review for journal The Cryosphere
Published: 30 March 2016

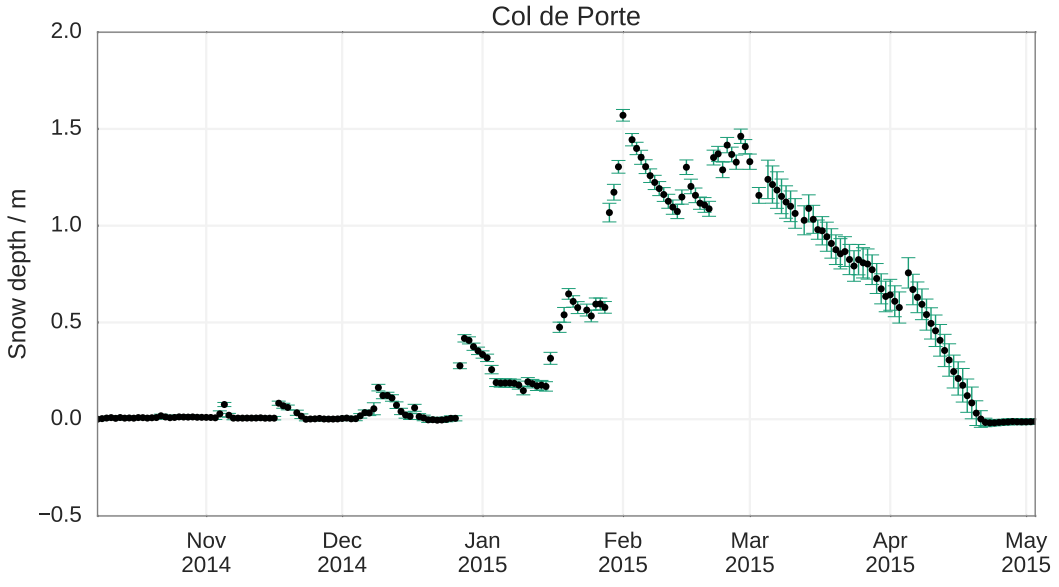

Figure 3. Evolution of the mean (black) and standard deviation (green) of the snow depth at Col de Porte over the winter season 2014 – 2015 measured by the RLS.

The Cryosphere Discuss., doi:10.5194/tc-2016-67, 2016
Manuscript under review for journal The Cryosphere
Published: 30 March 2016

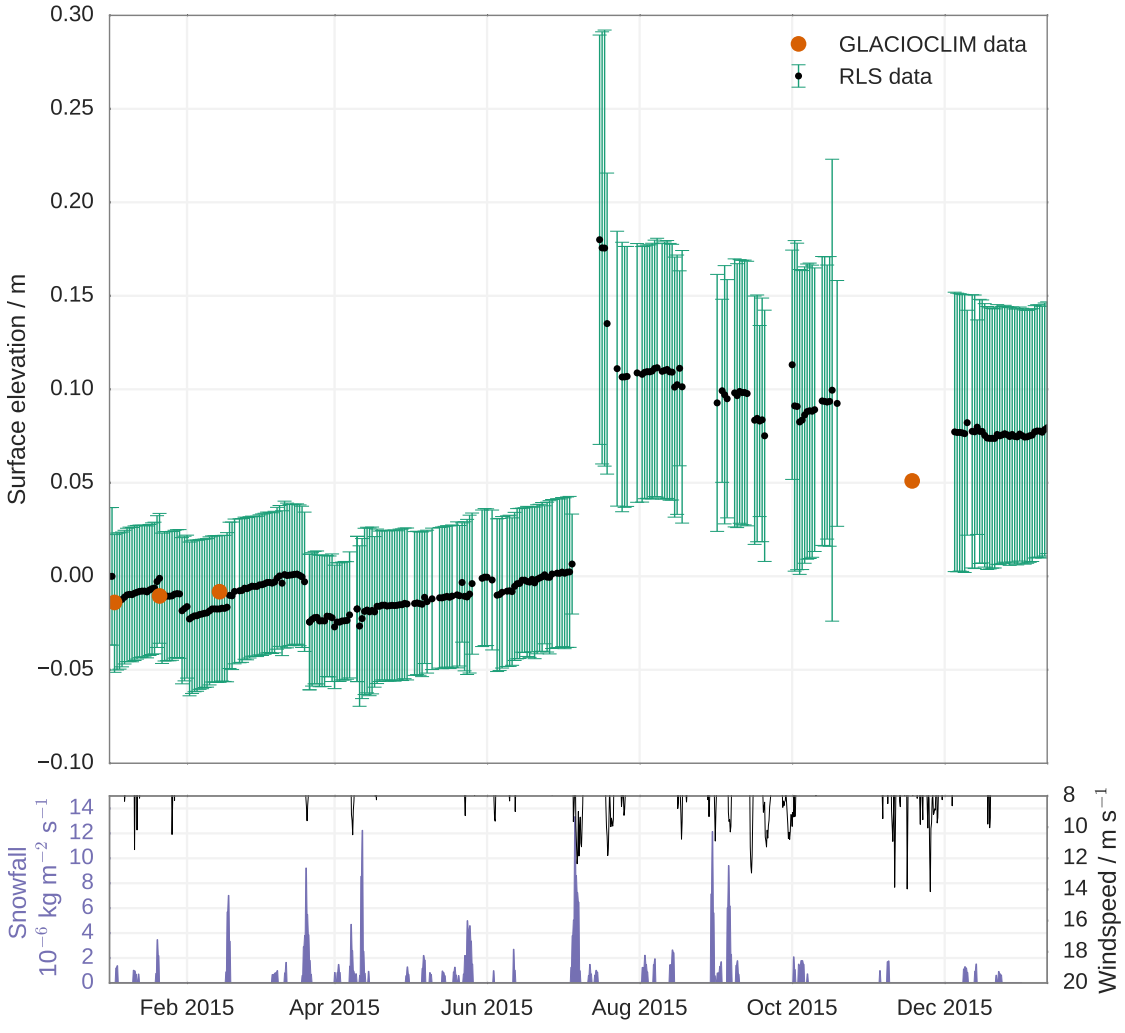

Figure 4. Evolution of the mean (black) and standard deviation (green) of the surface elevation change at Dome C in 2015 and January 2016 measured by the RLS. Orange points show the mean accumulation deduced from emergence measurements of the GLACIOCLIM 50-stack network. The reference is calculated so that the first GLACIOCLIM measurement (3 January 2015) equals the mean RLS snow elevation measured the same day.

The Cryosphere Discuss., doi:10.5194/tc-2016-67, 2016
Manuscript under review for journal The Cryosphere
Published: 30 March 2016

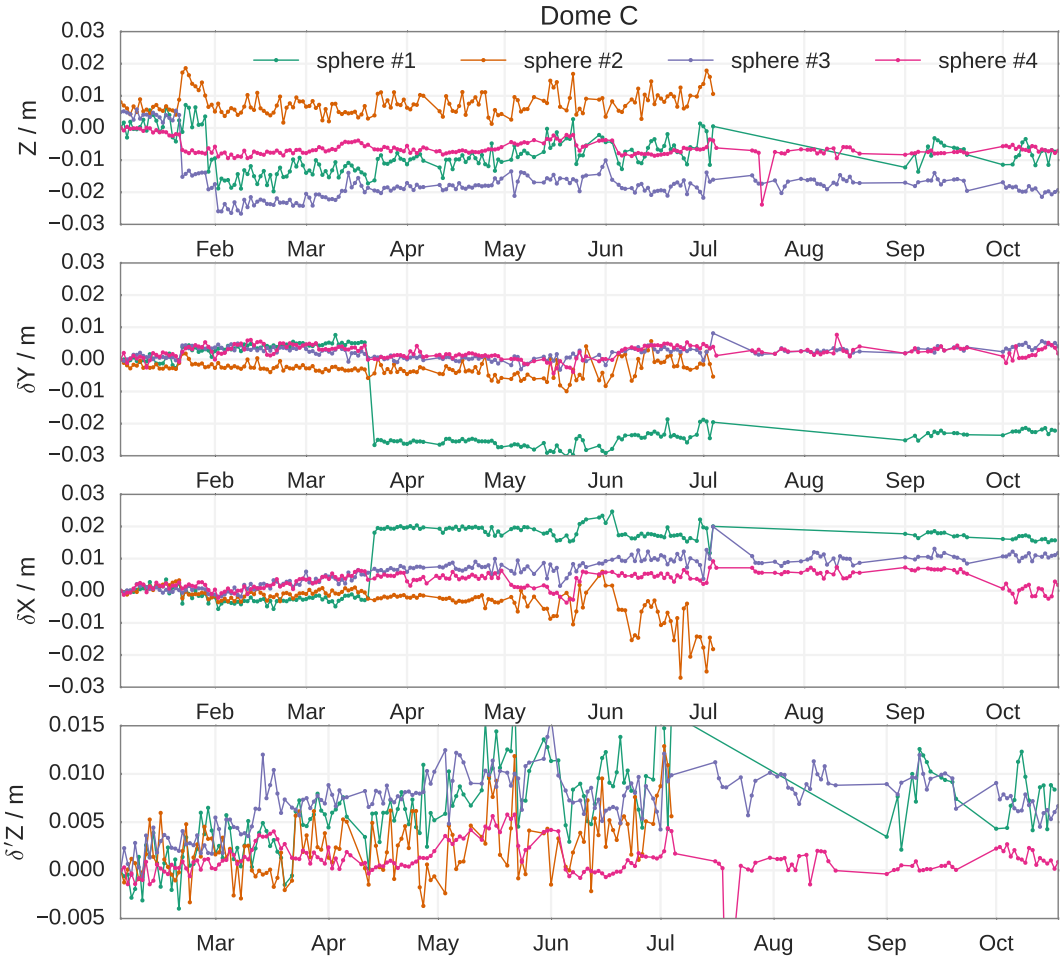

Figure 5. Evolution of the 4 reference spheres coordinates (x, y, z) at Dome C. δ and δ' respectively refer to the changes with respect to the first scan (1st January 2015) and to a scan just after a period of settling (1st February 2015).

The Cryosphere Discuss., doi:10.5194/tc-2016-67, 2016
Manuscript under review for journal The Cryosphere
Published: 30 March 2016

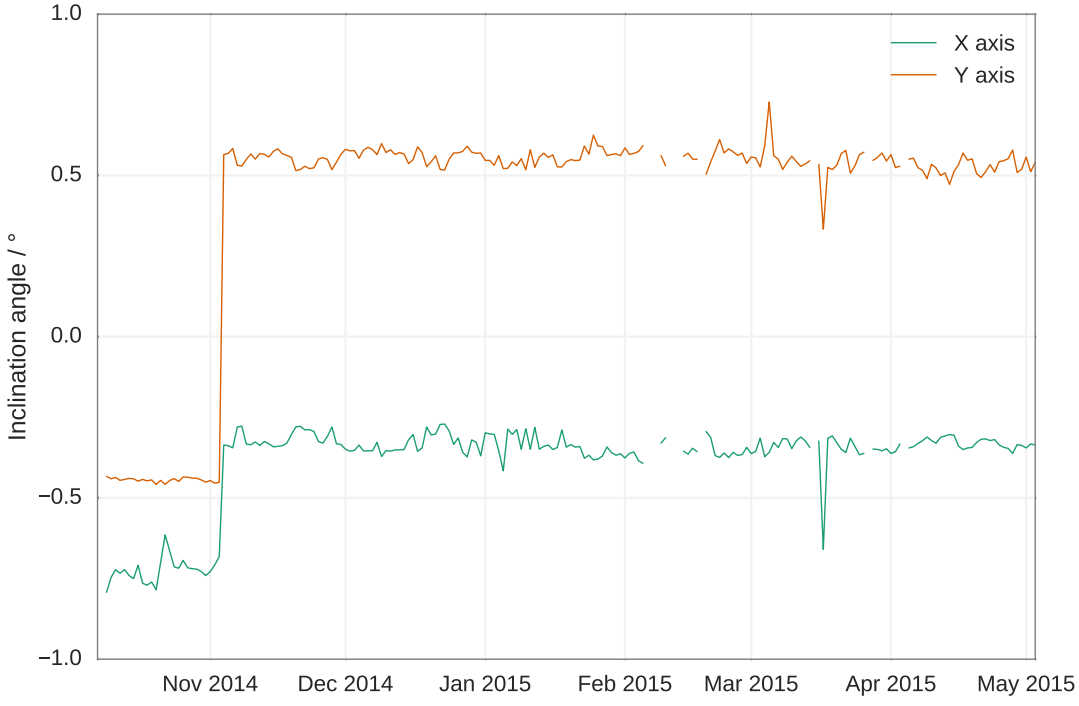

Figure 6. Evolution of the inclination of the laser over the season at Col de Porte.

The Cryosphere Discuss., doi:10.5194/tc-2016-67, 2016
Manuscript under review for journal The Cryosphere
Published: 30 March 2016

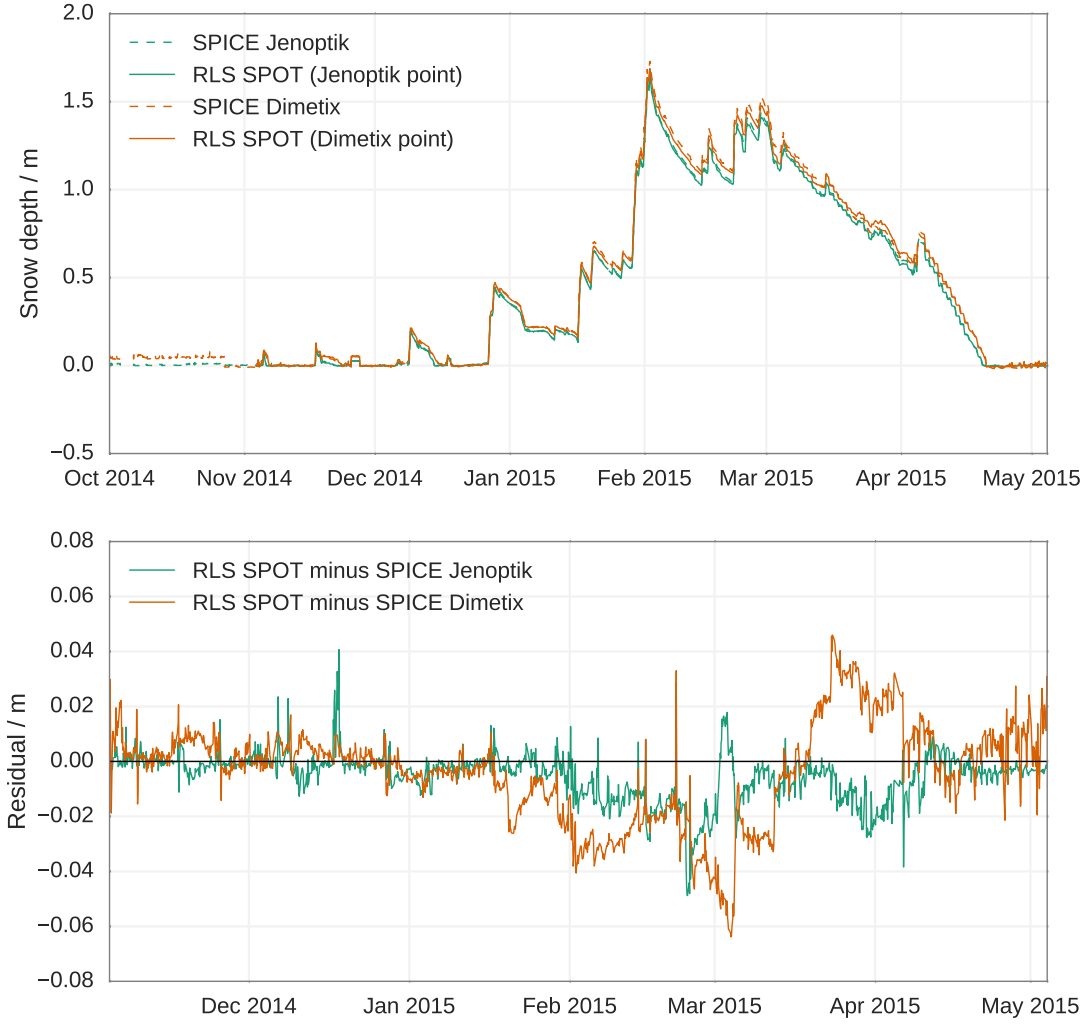

Figure 7. Evaluation of the RLS spot mode against SPICE lasermeters at Col de Porte. Top panel shows the depth, bottom panel differences between sensors.

The Cryosphere Discuss., doi:10.5194/tc-2016-67, 2016
Manuscript under review for journal The Cryosphere
Published: 30 March 2016

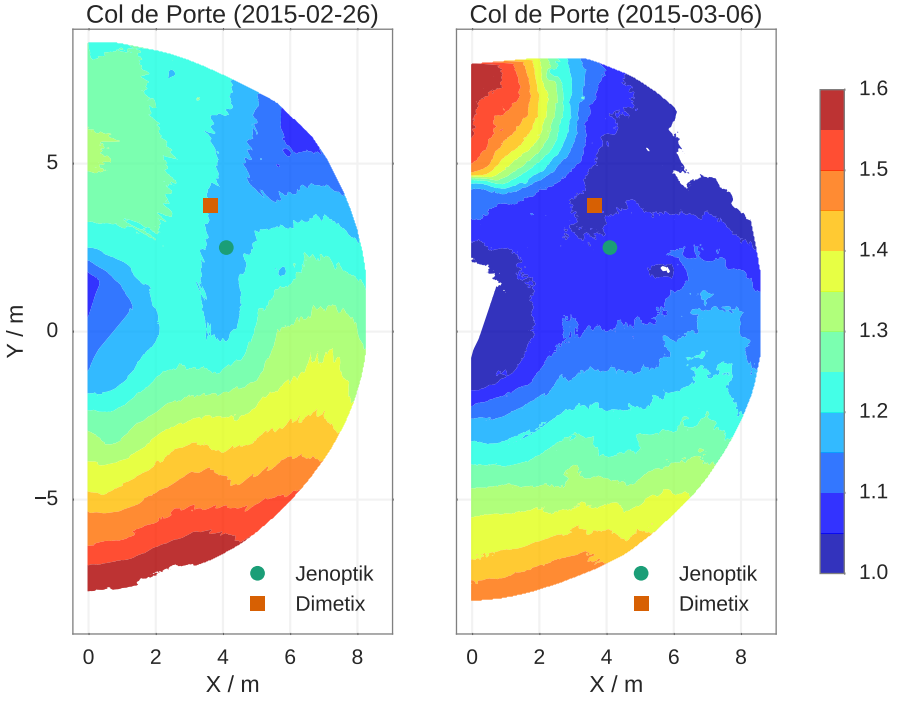

Figure 8. Two snow depth maps acquired at Col de Porte 26 February 2015 when the snow depth reaches its maximum and 6 March 2015 after a windslab appeared in the North corner $(x, y) \approx (0, 6\,\mathrm{m})$. The square and round symbols represent the footprint of the SPICE sensors at the beginning of the season.

The Cryosphere Discuss., doi:10.5194/tc-2016-67, 2016
Manuscript under review for journal The Cryosphere
Published: 30 March 2016

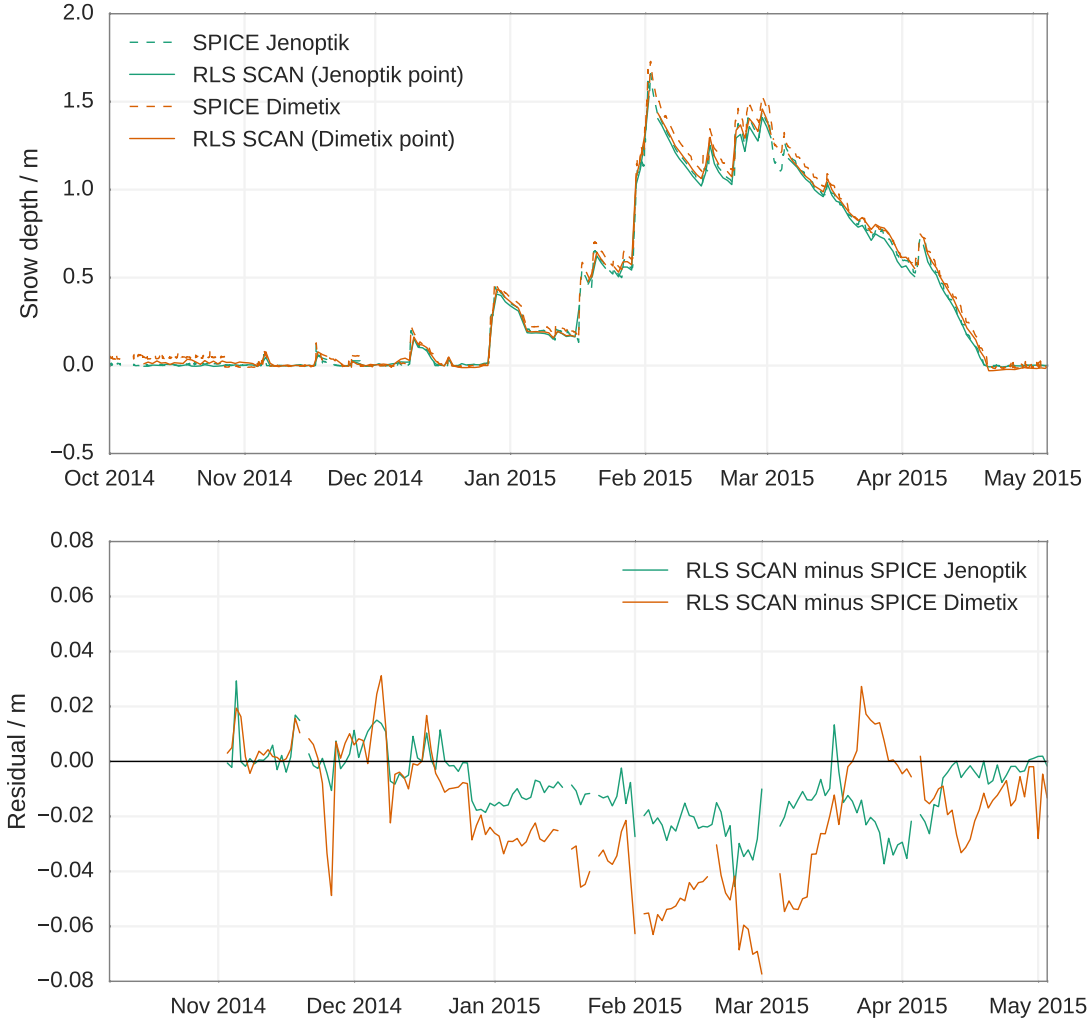

Figure 9. Evaluation of the RLS scan mode against SPICE lasermeters.

The Cryosphere Discuss., doi:10.5194/tc-2016-67, 2016
Manuscript under review for journal The Cryosphere
Published: 30 March 2016

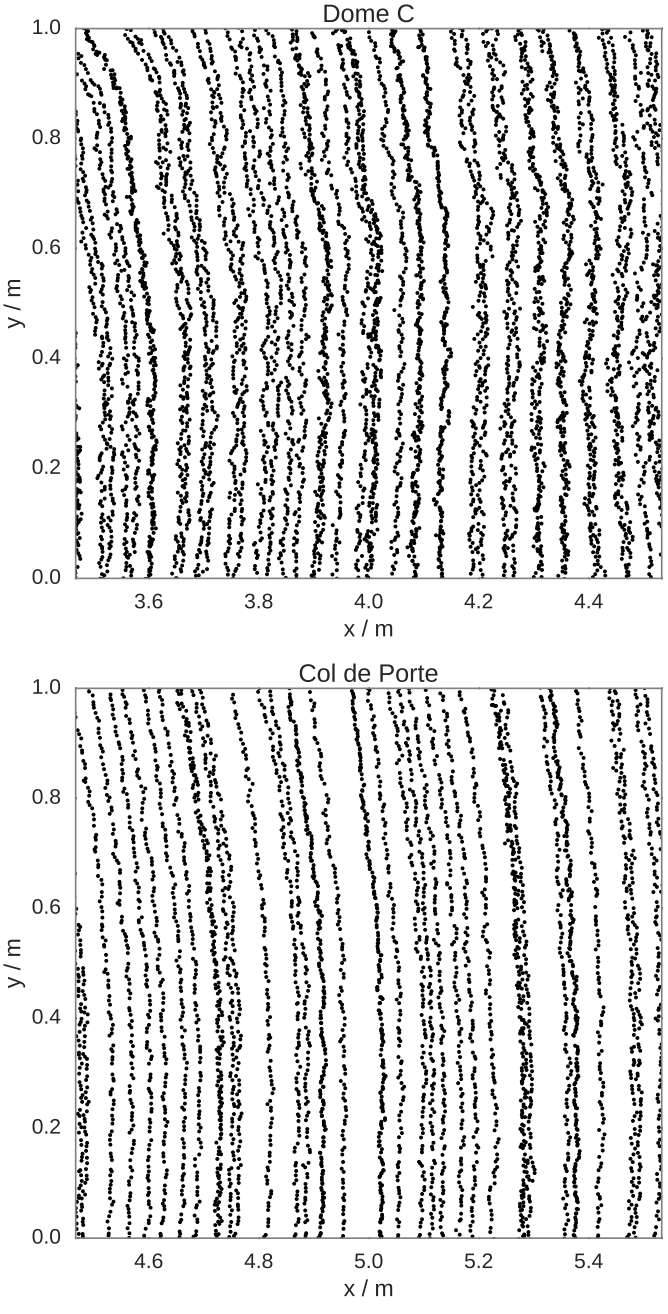

Figure 10. Zoom of the scans at Dome C and Col de Porte acquired 15 February 2015. Each point shown in the (x,y) plan is an individual measurement of the lasermeter.

The Cryosphere Discuss., doi:10.5194/tc-2016-67, 2016
Manuscript under review for journal The Cryosphere
Published: 30 March 2016

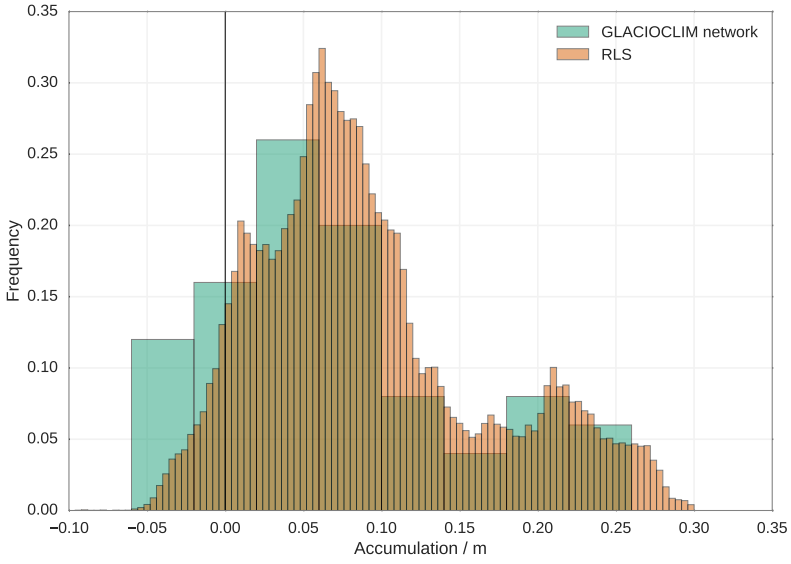

Figure 11. Distribution of the spatial variations of accumulation at Dome C observed by RLS (measured between 3 January 2015 and 5 December 2015) and the GLACIOCLIM network at 2 km from Concordia station (measured between 3 January and 18 November 2015).

The Cryosphere Discuss., doi:10.5194/tc-2016-67, 2016
Manuscript under review for journal The Cryosphere
Published: 30 March 2016

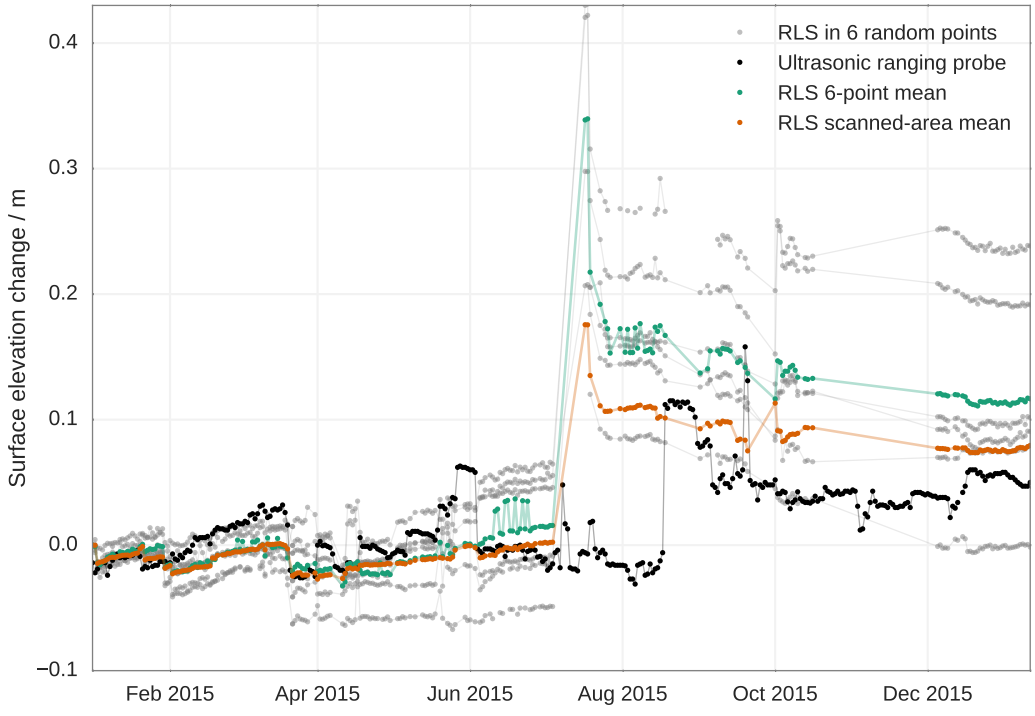

Figure 12. Evolution of the snow surface elevation change at Dome C taken in 6 random points in the scanned area (gray), on average over the 6 points (green), on average over the scanned area (orange), and measured by a nearby ultrasonic ranging probe (black).